Advanced MHD models of anisotropy, flow and chaotic fields

M. J. Hole[1], M. Fitzgerald[1,4], G. Dennis[1], Zhisong Qu[1],
S. Hudson[2], R. L. Dewar[1], D. Terranova[3], L. C. Appel[4],
P. Franz[3], G. von Nessi[1] , B. Layden[1]

[1] Australian National University, ACT 0200, Australia

[2] Princeton Plasma Physics Laboratory, New Jersey 08543, U.S.A.

[3] Consorzio RFX, Padua, Italy

[4] EURATOM/CCFE Fusion Assoc., Culham Science Centre,Abingdon, Oxon OX14 3DB, UK

42nd EPS Conference on Plasma Physics

21-26 June 2015

Funding Acknowledgement: Australian Research Council, DIISRTE
Support Acknowledgement: Luca Guazzotto (University of Rochester), David Pretty (ANU), Rob Akers, Ken McClements, David Muir (CCFE)

MHD with rotation & anisotropy

- Inclusion of anisotropy and flow in equilibrium MHD equations

[R. Iacono, et al Phys. Fluids B 2 (8). 1990]

$$\nabla \cdot (\rho \mathbf{v}) = 0, \qquad \rho \mathbf{v} \cdot \nabla \mathbf{v} = \mathbf{J} \times \mathbf{B} - \nabla \cdot \overline{\mathbf{P}}, \qquad \nabla \cdot \mathbf{B} = 0$$

$$\mu_0 \mathbf{J} = \nabla \times \mathbf{B}, \qquad \nabla \times (\mathbf{v} \times \mathbf{B}) = 0,$$

$$\overline{\mathbf{P}} = p_\perp \overline{\mathbf{I}} + \Delta \mathbf{B}\mathbf{B} / \mu_0 , \qquad \Delta = \frac{\mu_0 (p_{||} - p_\perp)}{B^2}$$

MHD with rotation & anisotropy

- Inclusion of anisotropy and flow in equilibrium MHD equations

[R. Iacono, et al Phys. Fluids B 2 (8). 1990]

$$\nabla\cdot(\rho\mathbf{v})=0,\qquad \rho\mathbf{v}\cdot\nabla\mathbf{v}=\mathbf{J}\times\mathbf{B}-\nabla\cdot\overline{\mathbf{P}},\qquad \nabla\cdot\mathbf{B}=0$$

$$\mu_0\mathbf{J}=\nabla\times\mathbf{B},\qquad \nabla\times(\mathbf{v}\times\mathbf{B})=0,$$

$$\overline{\mathbf{P}}=p_\perp\overline{\mathbf{I}}+\Delta\mathbf{BB}/\mu_0\,,\qquad \Delta=\frac{\mu_0\left(p_{||}-p_\perp\right)}{B^2}$$

- Frozen flux condition + axis-symmetry + neglect poloidal flow $\Rightarrow$

$$\mathbf{v}=-R\phi_E'(\psi)\mathbf{e}_\varphi=R\Omega(\psi)\mathbf{e}_\varphi$$

Equilibrium eqn becomes:

$$\boxed{\nabla\cdot\left[(1-\Delta)\left(\frac{\nabla\psi}{R^2}\right)\right]=-\frac{\partial p_{||}}{\partial\psi}-\rho H'(\psi)+\rho\frac{\partial W}{\partial\psi}-\frac{F(\psi)F'(\psi)}{R^2(1-\Delta)}+R^2\rho\Omega(\psi)\Omega'(\psi)}$$

$$F=RB_\varphi\qquad H(\psi)=W_M(\rho,B,\psi)-\frac{1}{2}\left[R\phi_E'(\psi)\right]^2$$

Guiding-centre/MHD/double-adiabatic

MHD with rotation & anisotropy

- Inclusion of anisotropy and flow in equilibrium MHD equations

[R. Iacono, et al Phys. Fluids B 2 (8). 1990]

$$\nabla\cdot(\rho\mathbf{v})=0, \qquad \rho\mathbf{v}\cdot\nabla\mathbf{v}=\mathbf{J}\times\mathbf{B}-\nabla\cdot\overline{\mathbf{P}}, \qquad \nabla\cdot\mathbf{B}=0$$

$$\mu_0\mathbf{J}=\nabla\times\mathbf{B}, \qquad \nabla\times(\mathbf{v}\times\mathbf{B})=0,$$

$$\overline{\mathbf{P}}=p_\perp\overline{\mathbf{I}}+\Delta\mathbf{BB}/\mu_0\,, \qquad \Delta=\frac{\mu_0\left(p_{||}-p_\perp\right)}{B^2}$$

- Frozen flux condition + axis-symmetry + neglect poloidal flow $\Rightarrow$

$$\mathbf{v}=-R\phi_E'(\psi)\mathbf{e}_\varphi=R\Omega(\psi)\mathbf{e}_\varphi$$

Equilibrium eqn becomes:

$$\boxed{\nabla\cdot\left[(1-\Delta)\left(\frac{\nabla\psi}{R^2}\right)\right]=-\frac{\partial p_{||}}{\partial\psi}-\rho H'(\psi)+\rho\frac{\partial W}{\partial\psi}-\frac{F(\psi)F'(\psi)}{R^2(1-\Delta)}+R^2\rho\Omega(\psi)\Omega'(\psi)}$$

$$F=RB_\varphi \qquad H(\psi)=W_M(\rho,B,\psi)-\frac{1}{2}\left[R\phi_E'(\psi)\right]^2$$

Guiding-centre/MHD/double-adiabatic

- If two temperature Bi-Maxwellian model chosen

$$p_{||}(\rho,B\psi)=\frac{k_B}{m}\rho T_{||}(\psi) \qquad p_\perp(\rho,B\psi)=\frac{k_B}{m}\rho T_\perp(\psi)=\frac{k_B}{m}\rho T_{||}(\psi)\frac{B}{B-\theta(\psi)T_{||}}$$

Set of 5 profile constraints $\{F(\psi),\Omega(\psi),H(\psi),T_{||}(\psi),\theta(\psi)\}$

EFIT TENSOR: reconstruction code

- Adds kinetic constraints to magnetic-only constraints of EFIT
- Soloviev benchmarks computed for isotropic, anisotropic and flow
  (Reveals J_ϕ sensitive to heat transport constraints)
- Installed for both MAST and JET

[Fitzgerald, Appel, Hole, Nucl. Fusion **53** (2013) 113040]

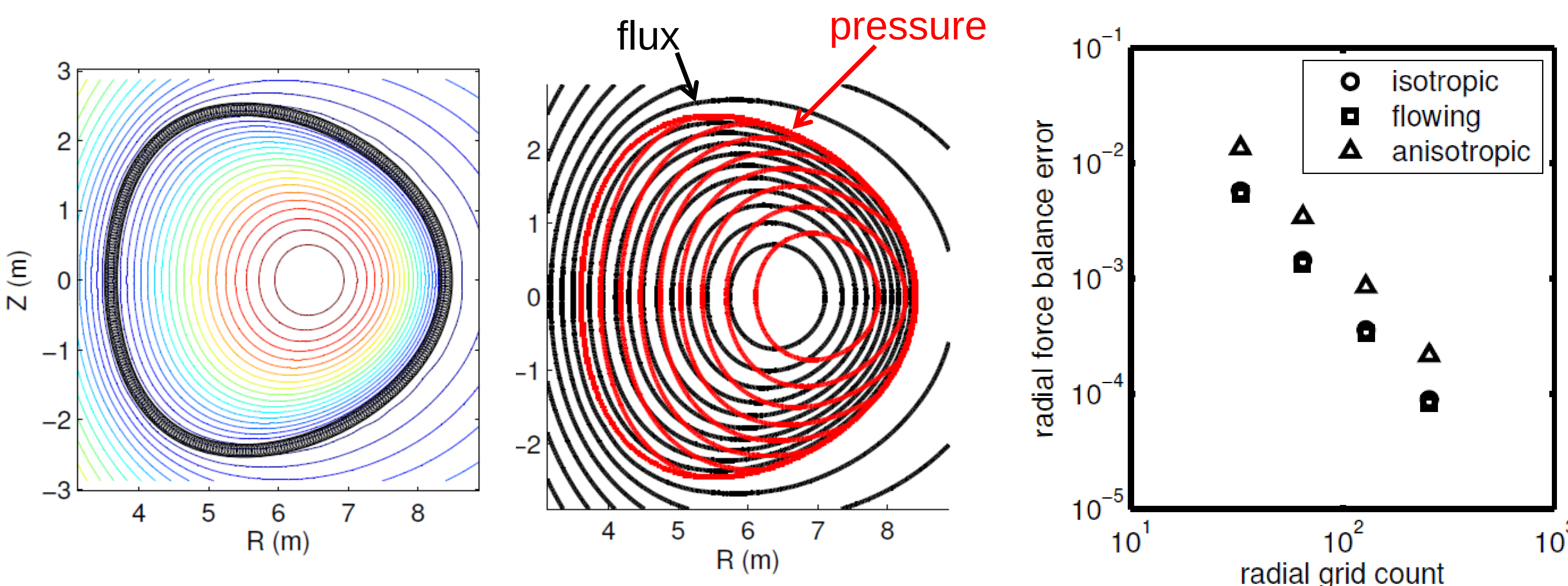

Soloviev:
β_t=0.07

Extended Soloviev:
β_t=0.07, M_ϕ=0.8, Δ=-0.004,

Solution Convergence

J_ϕ a strong function of transport model

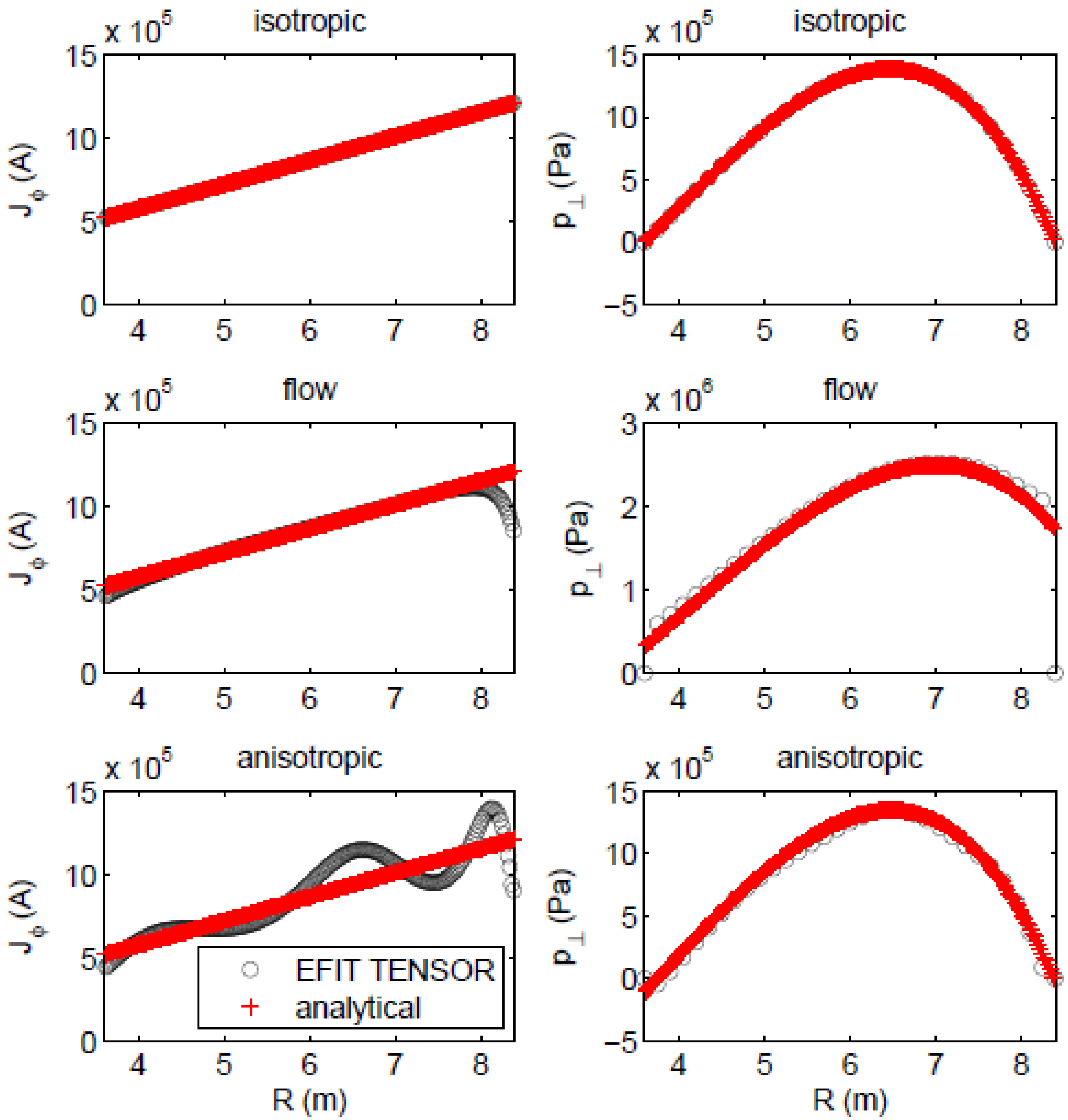

e.g. ITER-like plasma

ϵ	0.4
σ	1
τ	1
R_0	6 m
B_0	5 T
α	-3
ρ_0	1×10^{-7}
Ω_0	0 or $7 \times 10^5 \mathrm{rad\ s}^{-1}$
Δ_0	0 or 4×10^{-3}
I_p	16 MA
q^*	1.6
β_p	1.0
β_T	0.07

$p_\perp / p_{||} \sim 1.06$

Extended Soloviev

$$p_\perp(R,B,\psi) = \frac{1}{2}\rho_0\Omega_0^2R^2 - \frac{\Delta_0}{2}B^2 + \sigma_0 p_S(\psi)$$

$$p_\parallel(R,B,\psi) = \frac{1}{2}\rho_0\Omega_0^2R^2 + \frac{\Delta_0}{2}B^2 + \sigma_0 p_S(\psi)$$

EFIT TENSOR

$$p_\perp(\rho, B\psi) = \frac{k_B}{m}\rho T_\perp(\psi)$$

$$p_\parallel(\rho, B\psi) = \frac{k_B}{m}\rho T_\parallel(\psi)$$

HELENA+ATF

Zhisong Qu

- Companion code written to enable stability studies.
- Can be used to study how equilibrium changes with anisotropy

$$J_\varphi = \underbrace{R\frac{B_p^2}{B^2}\left(\frac{\partial p_\parallel}{\partial \Psi}\right)_B}_{p_\parallel} + \underbrace{R\frac{B^2-B_p^2}{B^2}\left(\frac{\partial p_\perp}{\partial \Psi}\right)_B}_{p_\perp} + \underbrace{\frac{1-\Delta}{2R}\left(\frac{\partial (RB_\varphi)^2}{\partial \Psi}\right)_B}_{toroidal\,field} \underbrace{- R\nabla\cdot\frac{\Delta\nabla\Psi}{R^2}}_{nonlinear}$$

HELENA+ATF

Zhisong Qu

- Companion code written to enable stability studies.
- Can be used to study how equilibrium changes with anisotropy

$$J_\varphi = \underbrace{R\frac{B_p^2}{B^2}\left(\frac{\partial p_\parallel}{\partial\Psi}\right)_B}_{p_\parallel} + \underbrace{R\frac{B^2 - B_p^2}{B^2}\left(\frac{\partial p_\perp}{\partial\Psi}\right)_B}_{p_\perp} + \underbrace{\frac{1-\Delta}{2R}\left(\frac{\partial(RB_\varphi)^2}{\partial\Psi}\right)_B}_{toroidal\,field} - \underbrace{R\nabla\cdot\frac{\Delta\nabla\Psi}{R^2}}_{nonlinear}$$

MAST-like equilibrium

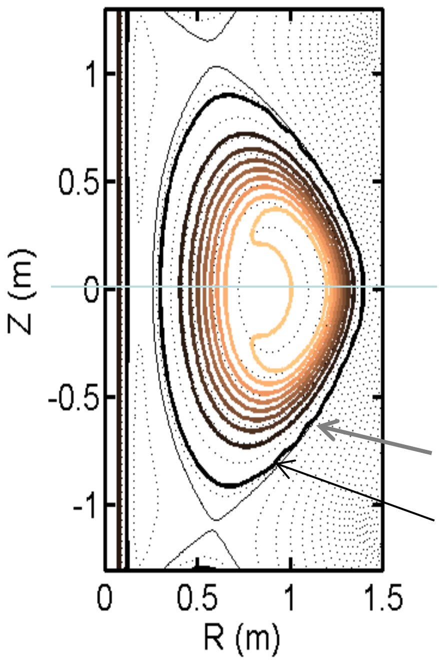

flux

surfaces of constant $p_{||}$.

J_ϕ components

$J_{\phi nl}$ core localised

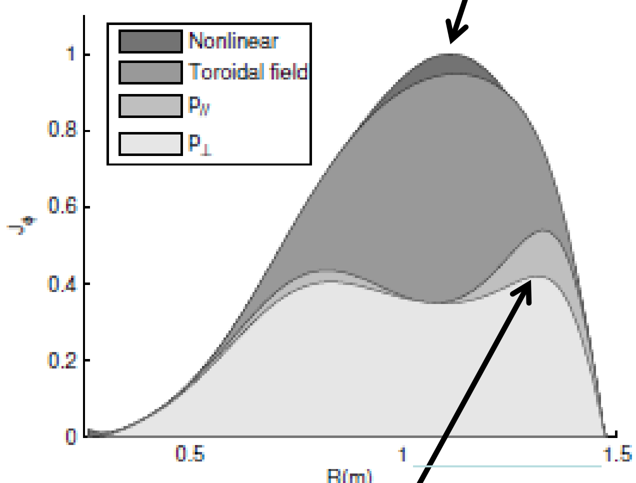

$J_{\phi ||}$ dominant outboard

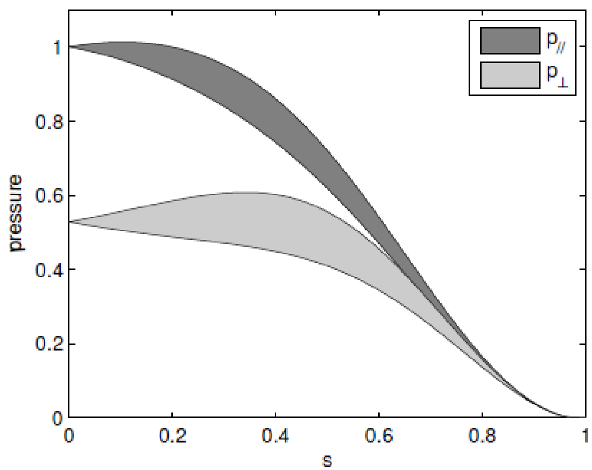

$s \propto \sqrt{r}$

[Qu, Fitzgerald, Hole, Plasma Phys. Control. Fusion **56** (2014) 075007]

Anisotropy modifies poloidal current

Zhisong Qu

- EFIT TENSOR reconstructions of MAST #18696 at 290ms
  - Anisotropic: $p_{||}$ and $p_{\perp}$ constrained to values from TRANSP
  - Isotropic: $p^* = (p_{||} + p_{\perp})/2$

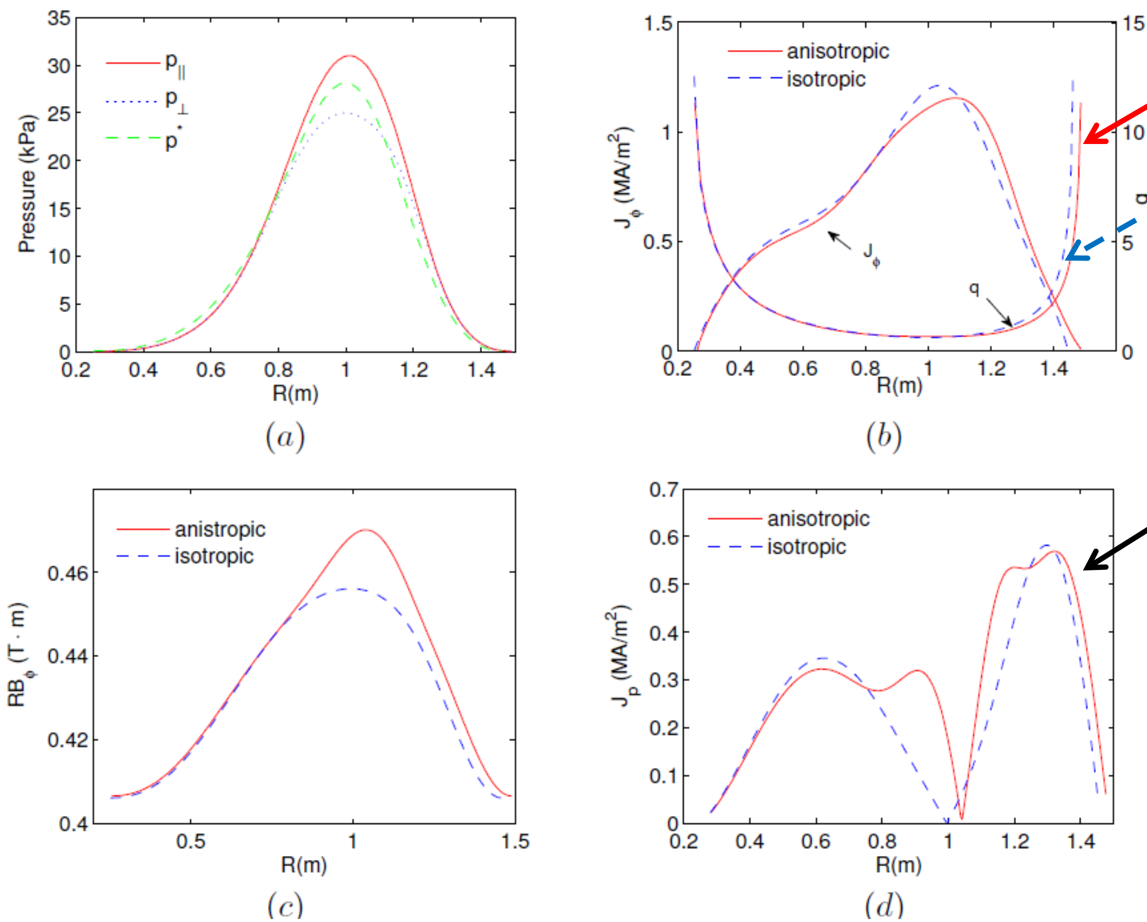

$p_{||}/p_{\perp} \approx 1.25$ (anisotropic)

$p^* = (p_{||} + p_{\perp})/2$ (isotropic)

Most significant difference in $\mathbf{J_p}$ which can effect change in stability

$$\mu_0 \boldsymbol{J_p} = \nabla(RB_\varphi) \times \nabla\varphi$$

Anisotropy on MAST: #29221

- MAST #29221
- 1.6MW NB heating
- I_p = 0.9MA, β_n~3
- Magnetics shows TAEs, tearing modes fishbones, long-lived modes

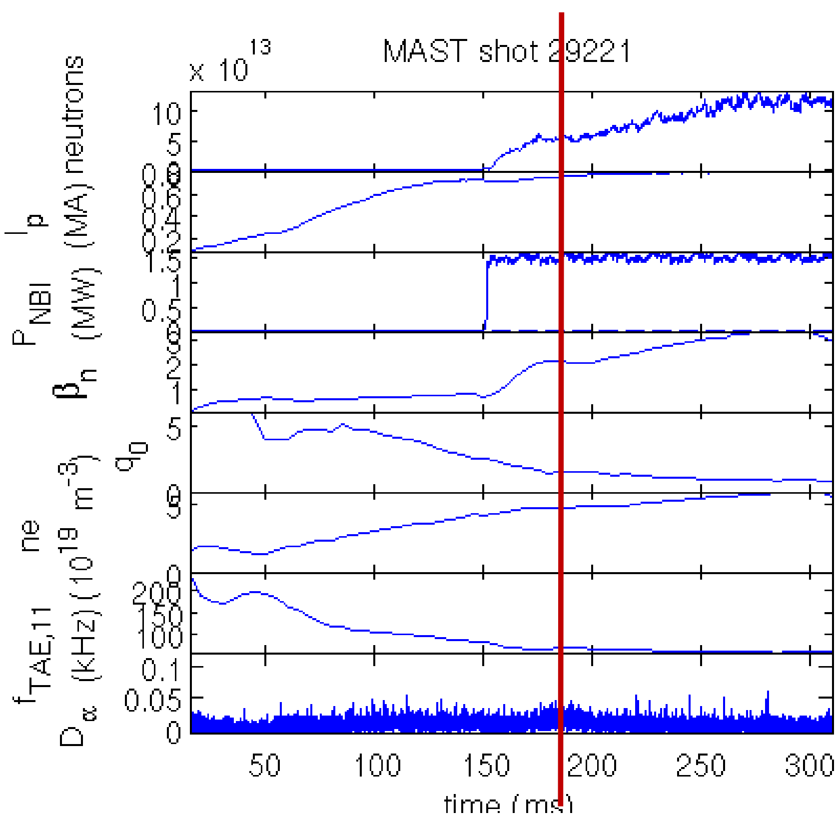

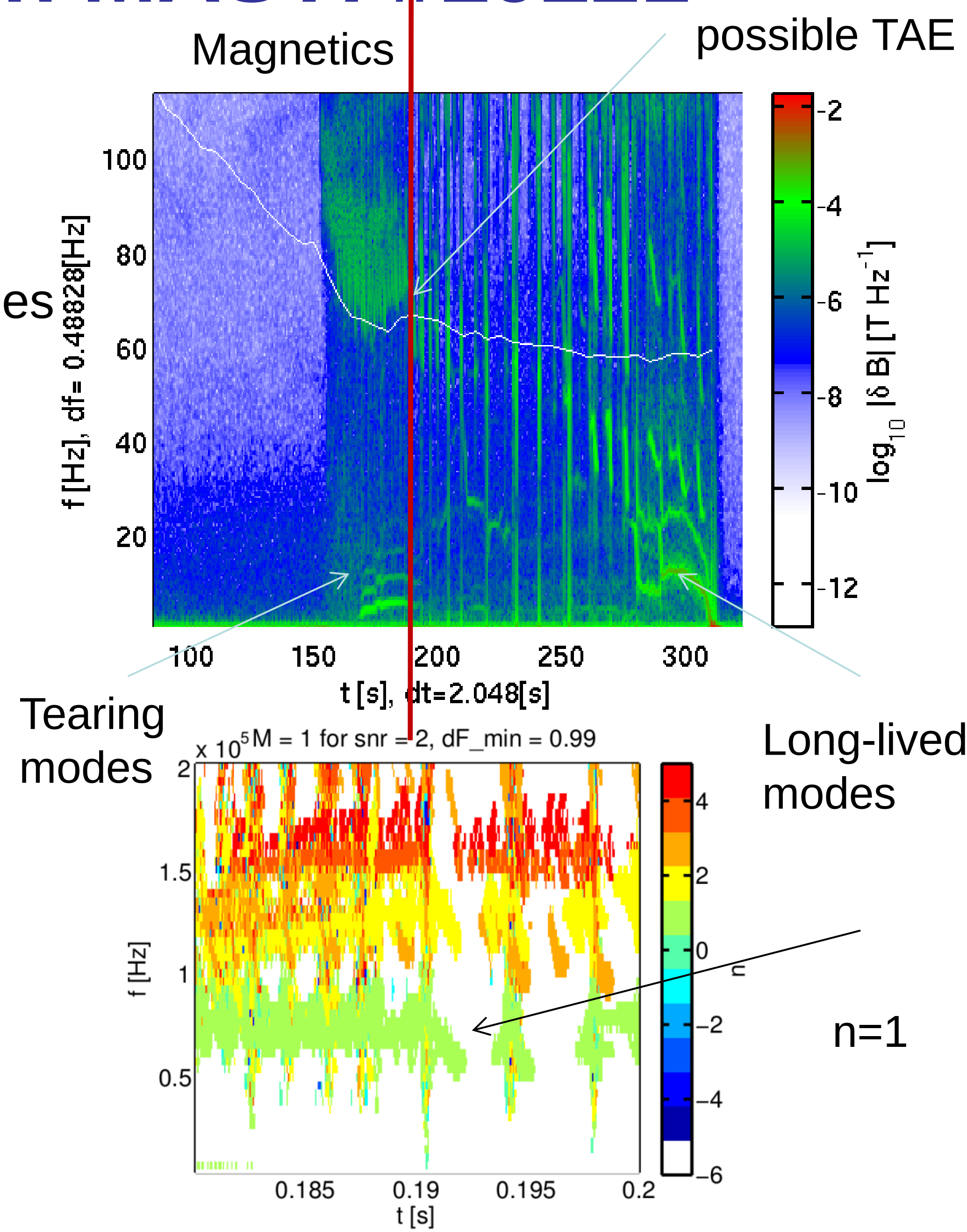

Beam + thermal population: $p_{\parallel} / p_{\perp} \approx 1.7$

HELENA+ATF / EFIT TENSOR: **p* = ($p_{\parallel}$+ $p_{\perp}$)/2 (isotropic)**

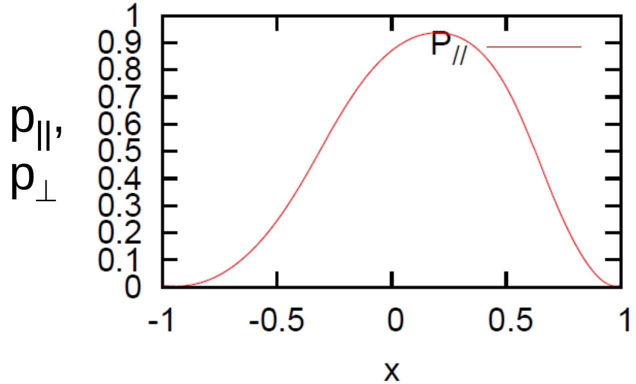

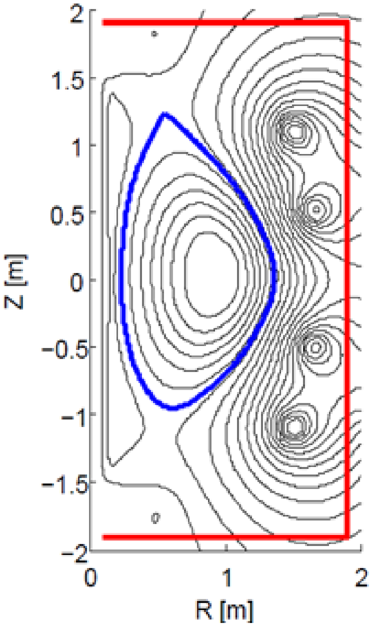

HELENA+ATF / EFIT TENSOR: **$p_{\parallel}$, $p_{\perp}$ (anisotropic)**

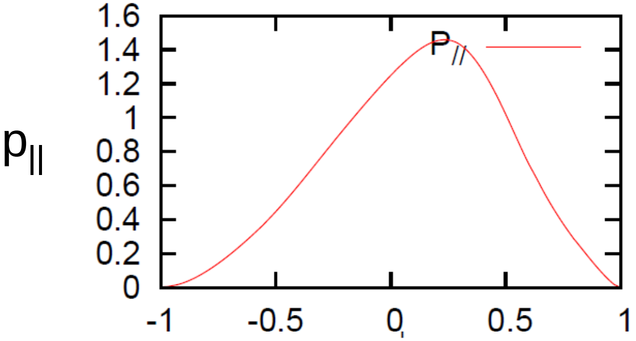

$p_{\parallel}/p_{\perp}$ = 1.7 at s=0.5 outboard

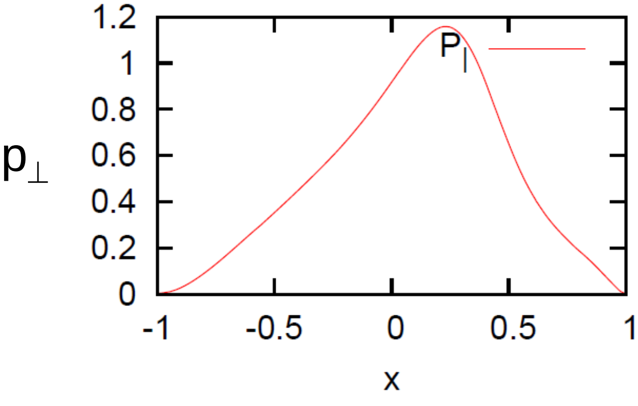

Beam + thermal population: $p_{||} / p_{\perp} \approx 1.7$

HELENA+ATF / EFIT TENSOR: **$p^* = (p_{||} + p_{\perp})/2$ (isotropic)**

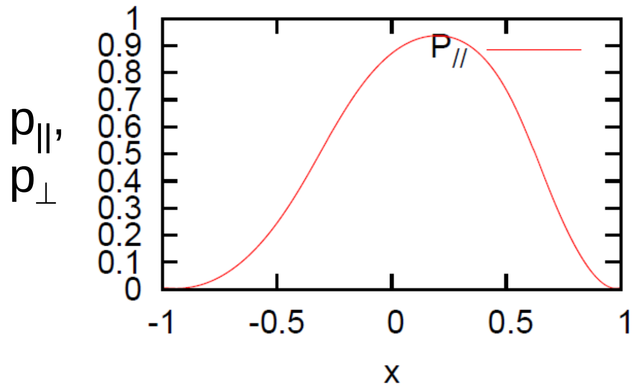

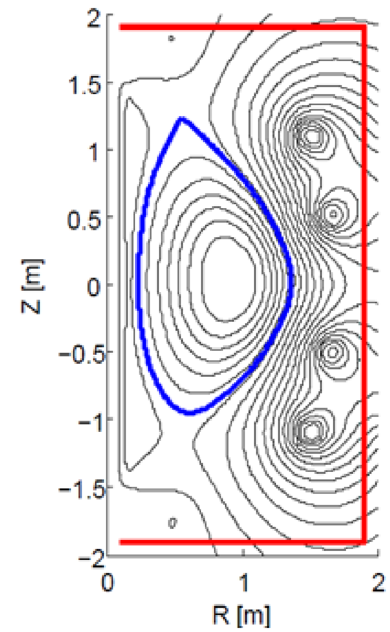

HELENA+ATF / EFIT TENSOR: **$p_{||}$, $p_{\perp}$ (anisotropic)**

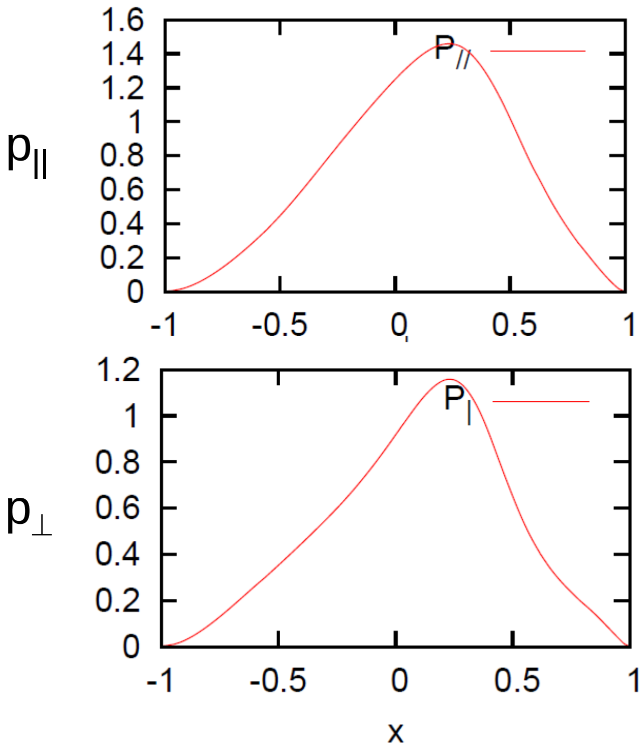

$p_{||}/p_{\perp}$ = 1.7 at s=0.5 outboard

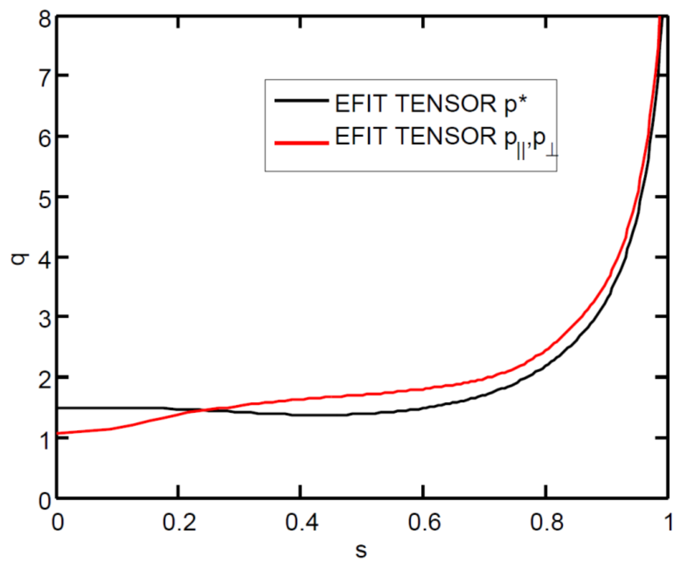

- What is the impact on stability due to this q profile?

Stability: New single adiabatic model

- Compressional
  - *Double-adiabatic (CGL)*
    - Collisionless, $p_\parallel$ and $p_\perp$ do **independent** work
    - No streaming particle heat flow
    - Does not reduce to MHD in the isotropic limit
  - *New Single adiabatic (SA) model*
    - $p_\parallel$ and $p_\perp$ doing **joint** work
    - Account for the isotropic part of the perturbation
    - Can reduce to MHD in isotropic limit
      [Fitzgerald, Hole, Qu, PPCF **57** (2015) 025018]

$$\frac{d}{dt}\left(\frac{p_\perp}{\rho B}\right) = 0,$$

$$\frac{d}{dt}\left(\frac{p_\parallel B^2}{\rho^3}\right) = 0.$$

$$\widetilde{\mathrm{P}} \to \tilde{p}\mathrm{I} + \widetilde{\pi}$$

$$\mathrm{Tr}\ \nabla \cdot \widetilde{Q} \to 0$$

$$\mathrm{Tr}\ \widetilde{\pi} \to 0$$

Stability: New single adiabatic model

- Compressional
  - *Double-adiabatic (CGL)*
    - Collisionless, $p_{\|}$ and $p_{\perp}$ do **independent** work
    - No streaming particle heat flow
    - Does not reduce to MHD in the isotropic limit

$$\frac{d}{dt}\left(\frac{p_{\perp}}{\rho B}\right) = 0,$$

$$\frac{d}{dt}\left(\frac{p_{\|} B^2}{\rho^3}\right) = 0.$$

  - *New Single adiabatic (SA) model*
    - $p_{\|}$ and $p_{\perp}$ doing **joint** work
    - Account for the isotropic part of the perturbation
    - Can reduce to MHD in isotropic limit
      [Fitzgerald, Hole, Qu, PPCF **57** (2015) 025018]

$$\widetilde{\mathrm{P}} \to \tilde{p}\mathrm{I} + \widetilde{\pi}$$

$$\mathrm{Tr}\ \nabla \cdot \widetilde{Q} \to 0$$

$$\mathrm{Tr}\ \widetilde{\pi} \to 0$$

- Incompressional

$$p_{\|_1} = -\xi_n \left[\frac{\partial p_{\|}}{\partial n} - (p_{\|} - p_{\perp})\frac{\partial \ln B}{\partial n}\right] \qquad p_{\perp 1} = -\xi_n \left[\frac{\partial p_{\perp}}{\partial n} - (2p_{\perp} + \hat{c})\frac{\partial \ln B}{\partial n}\right]$$

*A B Mikhailovskii, Instabilities in a confined plasma, IOP publishing (1998)

Stability: New single adiabatic model

- Compressional
  - *Double-adiabatic (CGL)*
    - Collisionless, $p_\parallel$ and $p_\perp$ do **independent** work
    - No streaming particle heat flow
    - Does not reduce to MHD in the isotropic limit

$$\frac{d}{dt}\left(\frac{p_\perp}{\rho B}\right) = 0,$$

$$\frac{d}{dt}\left(\frac{p_\parallel B^2}{\rho^3}\right) = 0.$$

  - *New Single adiabatic (SA) model*
    - $p_\parallel$ and $p_\perp$ doing **joint** work
    - Account for the isotropic part of the perturbation
    - Can reduce to MHD in isotropic limit

      [Fitzgerald, Hole, Qu, PPCF **57** (2015) 025018]

$$\widetilde{\mathrm{P}} \to \tilde{p}\mathrm{I} + \widetilde{\pi}$$

$$\mathrm{Tr}\ \nabla \cdot \widetilde{Q} \to 0$$

$$\mathrm{Tr}\ \widetilde{\pi} \to 0$$

- Incompressional

$$p_{\parallel 1} = -\xi_n \left[\frac{\partial p_\parallel}{\partial n} - (p_\parallel - p_\perp)\frac{\partial \ln B}{\partial n}\right] \qquad p_{\perp 1} = -\xi_n \left[\frac{\partial p_\perp}{\partial n} - (2p_\perp + \hat{c})\frac{\partial \ln B}{\partial n}\right]$$

*A B Mikhailovskii, Instabilities in a confined plasma, IOP publishing (1998)

- Implemented in CSCAS (CSMIS-A) and MISHKA (MISHKA-A)

  [Qu, Hole, Fitzgerald, PPCF submitted 09/02/2015]

MISHKA-A agrees with Bussac criterion

- Benchmark result Generalised Bussac condition: marginal stability of n=1 internal kink for ε=0.1, circular cross section

$$\frac{\langle p_{\perp}\rangle}{\langle p_{||}\rangle} = \frac{1}{1-\alpha(1-\psi_n)}$$

Bussac condition = solid lines
MISHKA-A = points

[Qu, Hole, Fitzgerald, PPCF submitted 09/02/2015]

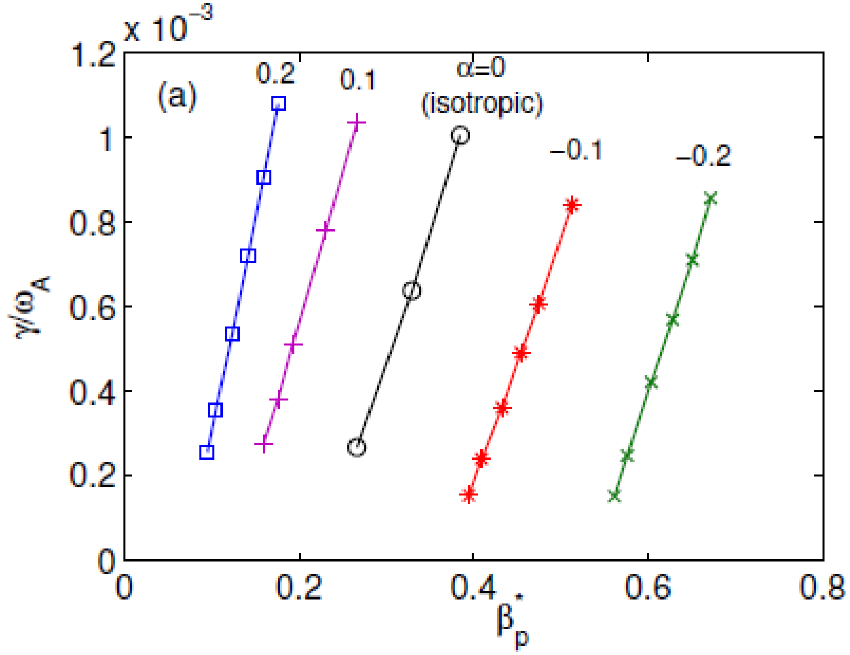

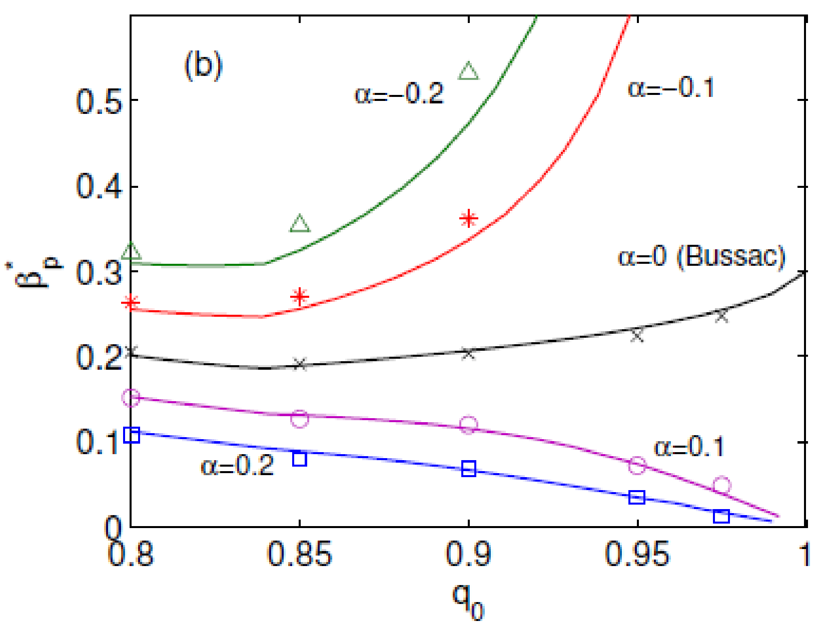

Incompressible continuum for MAST

isotropic

n=1, γ=0

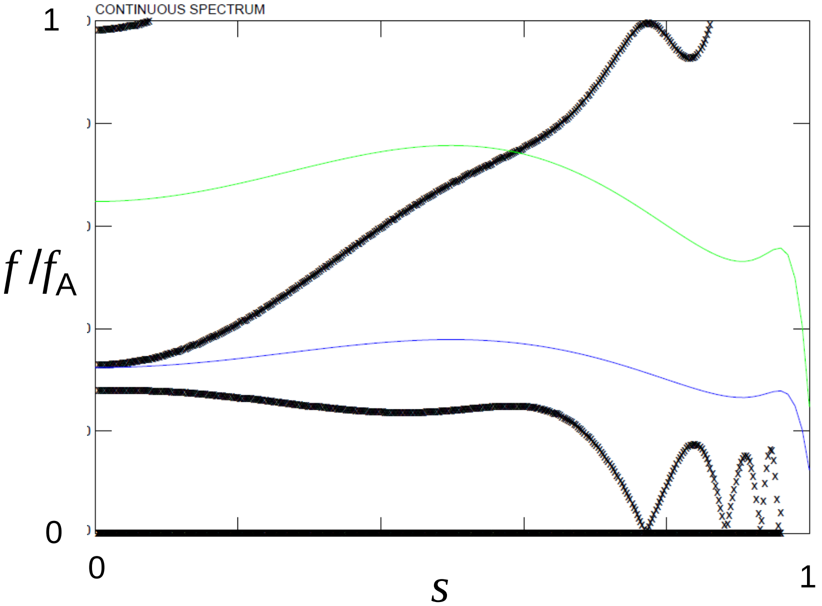

$R_{mag} = 0.914$

f_A at magnetic axis = 280kHz

Incompressible continuum for MAST

isotropic

n=1, γ=0

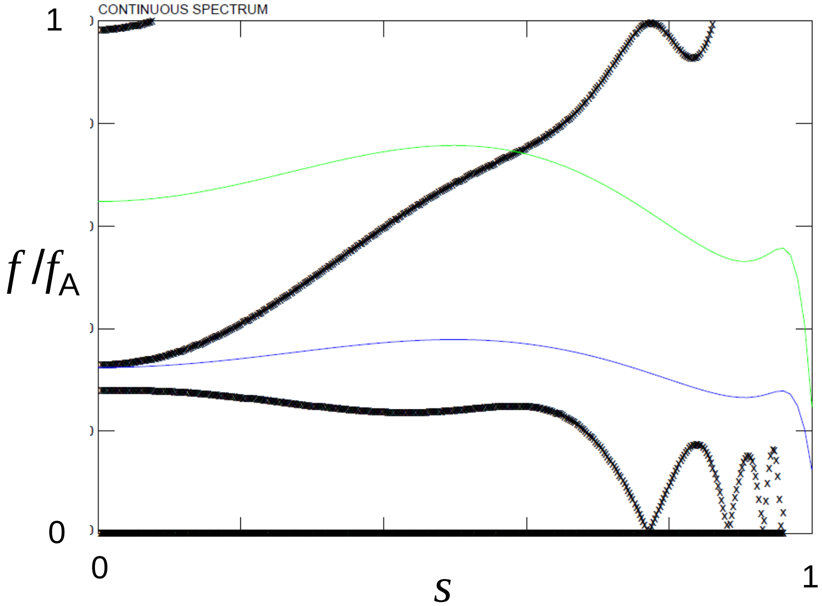

$R_{mag} = 0.914$

f_A at magnetic axis = 280kHz

anisotropic

n=1, γ=0

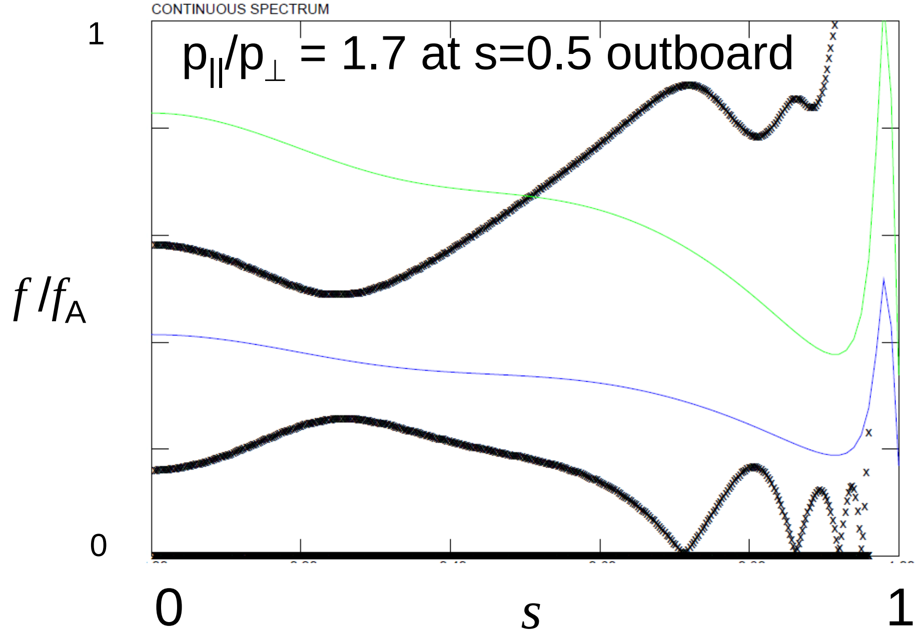

$R_{mag} = 0.928$

f_A at magnetic axis = 260kHz

isotropic Δf_{TAE} < anisotropic Δf_{TAE}

$\Rightarrow$anisotropic modes likely to have less continuum damping

mode profile broader with anisotropy

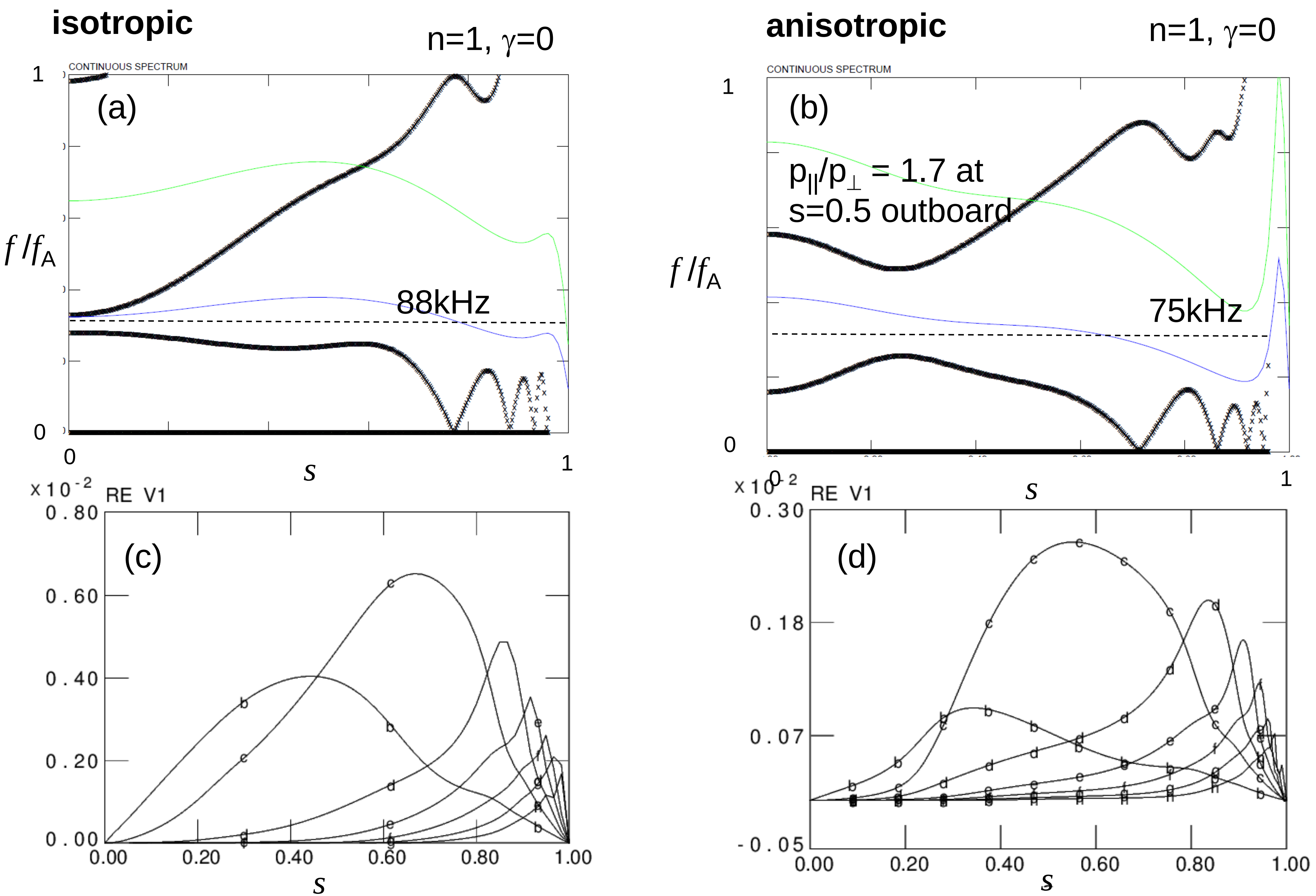

Ongoing work in Anisotropy and Flow

- What is the impact of different radial structure on anomalous transport?
  - Couple EFIT TENSOR, MISHKA-A to wave-particle interaction code HAGIS for self-consistent evolution
- Explore the impact of anisotropy and flow on a wide range of MAST plasma conditions

G. Bowden, A. Könies: Implemented complex contour algorithm into CKA to compute continuum damping in 3D

3D equilibria in toroidal plasmas

- Simplest model to approximate global, macroscopic force-balance is magnetohydrodynamics (MHD).

$$\nabla p = \mathbf{J} \times \mathbf{B}, \qquad \nabla \times \mathbf{B} = \mathbf{J}, \qquad \nabla \cdot \mathbf{B} = 0$$

3D equilibria in toroidal plasmas

- Simplest model to approximate global, macroscopic force-balance is magnetohydrodynamics (MHD).

$$\nabla p = \mathbf{J} \times \mathbf{B}, \qquad \nabla \times \mathbf{B} = \mathbf{J}, \qquad \nabla \cdot \mathbf{B} = 0$$

- Toroidal symmetry $\Rightarrow$ field lies in nested flux surfaces

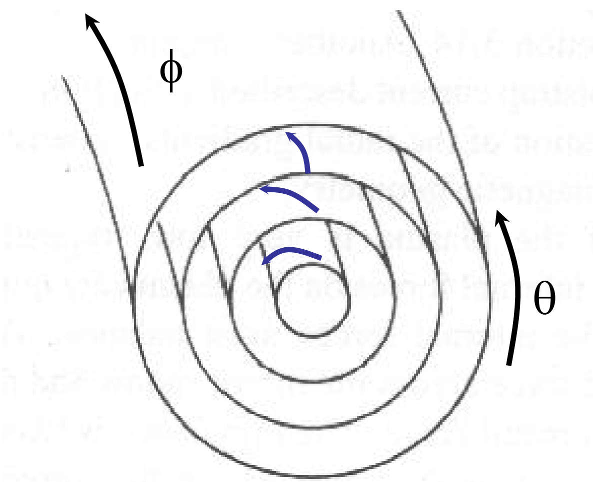

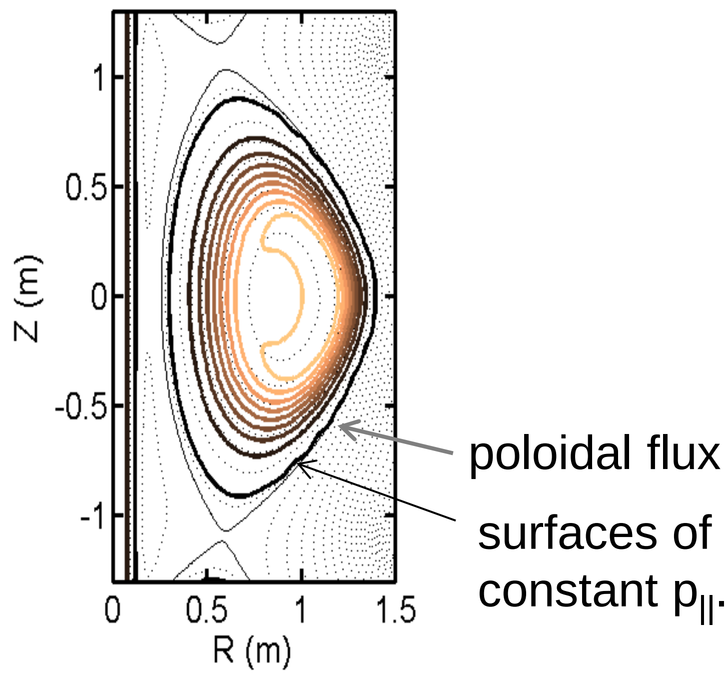

3D equilibria in toroidal plasmas

- Simplest model to approximate global, macroscopic force-balance is magnetohydrodynamics (MHD).

$$\nabla p = \mathbf{J} \times \mathbf{B}, \qquad \nabla \times \mathbf{B} = \mathbf{J}, \qquad \nabla \cdot \mathbf{B} = 0$$

- Non-axisymmetric $\Rightarrow$ field does **not** lie in nested flux surfaces **unless** surface currents allowed.

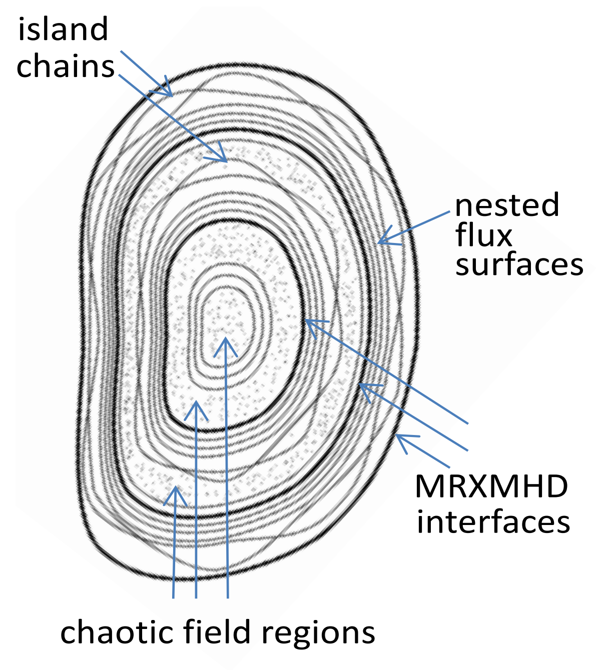

3D equilibria in toroidal plasmas

- Simplest model to approximate global, macroscopic force-balance is magnetohydrodynamics (MHD).

$$\nabla p = \mathbf{J} \times \mathbf{B}, \qquad \nabla \times \mathbf{B} = \mathbf{J}, \qquad \nabla \cdot \mathbf{B} = 0$$

- Non-axisymmetric $\Rightarrow$ field does **not** lie in nested flux surfaces **unless** surface currents allowed.
- Existing 3D solvers (e.g. VMEC) assume nested flux surfaces.

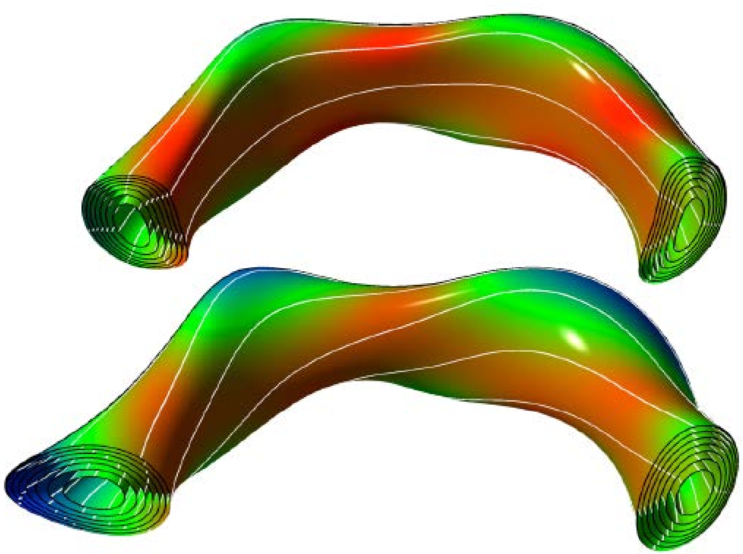

[CTH stellarator, Hanson et al, IAEA 2012]

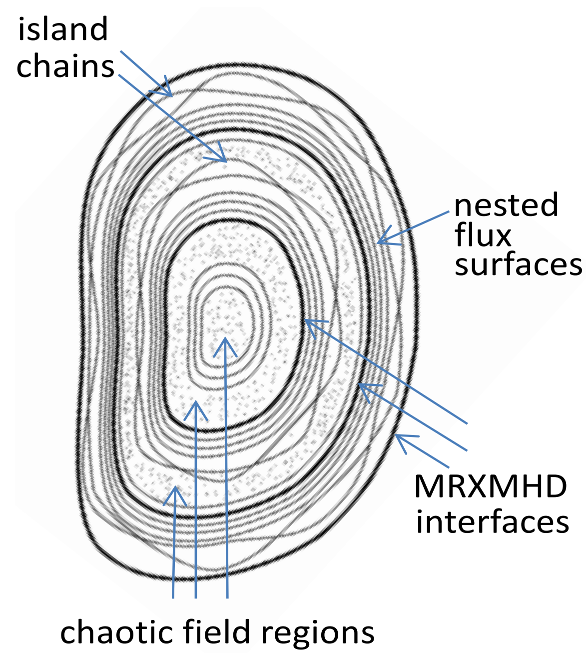

Generalised Taylor Relaxation:

Multiple Relaxed Region MHD (MRXMHD)

R. L. Dewar

- Assume each invariant tori I_i act as ideal MHD barriers to relaxation, so that Taylor constraints are localized to subregions.

New system comprises:

- N plasma regions P_i in relaxed states.
- Regions separated by ideal MHD barrier I_i.
- Enclosed by a vacuum V,
- Encased in a perfectly conducting wall W

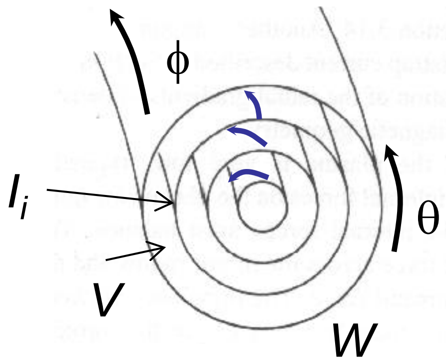

$$W_l = \int_{R_i} \left(\frac{B_l^{\,2}}{2\mu_0} + \frac{P_l}{\gamma - 1} \right) d\tau^3$$

$$H_l = \int_V (\mathbf{A}_l \cdot \mathbf{B}_l) d\tau^3$$

Seek minimum energy state:

$$F = \sum_{l=1}^{N} \left(W_l - \mu_l H_l / 2 \right)$$

$$P_l : \quad \nabla \times \mathbf{B} = \mu_l \mathbf{B}$$

$$P_l = \text{constant}$$

$$I_l : \quad \mathbf{B} \cdot \mathbf{n} = 0$$

$$[[P_l + B^2/(2\mu_0)]] = 0$$

$$V : \quad \nabla \times \mathbf{B} = 0$$

$$\nabla \cdot \mathbf{B} = 0$$

$$W : \quad \mathbf{B} \cdot \mathbf{n} = 0$$

MRXMHD approaches ideal MHD as N→∞

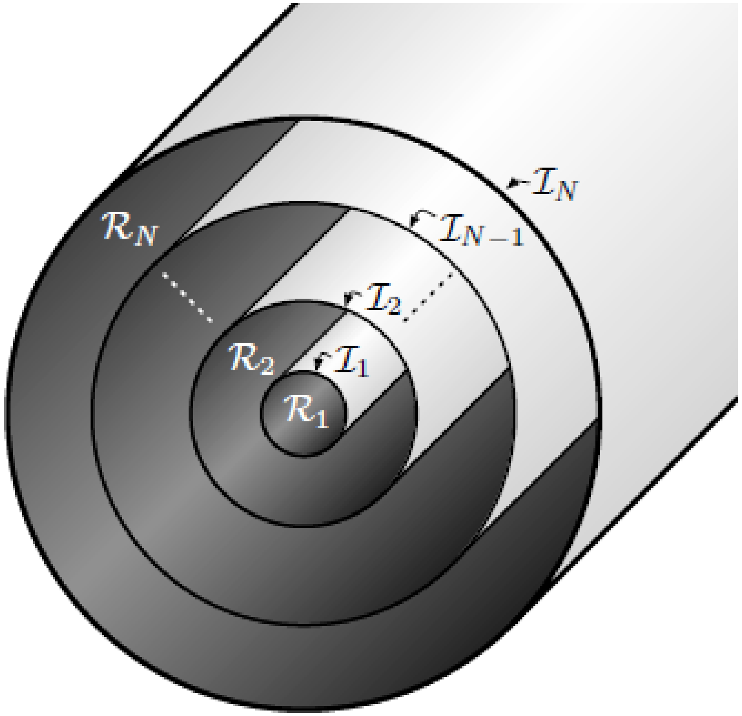

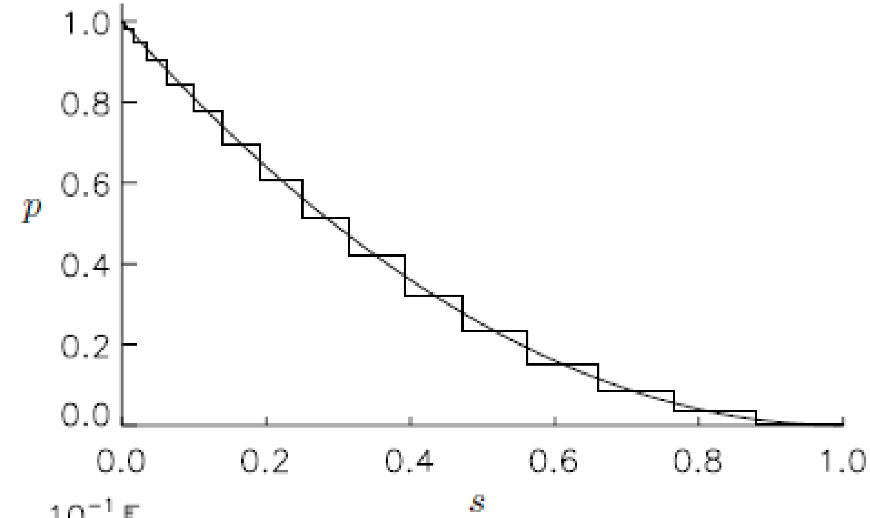

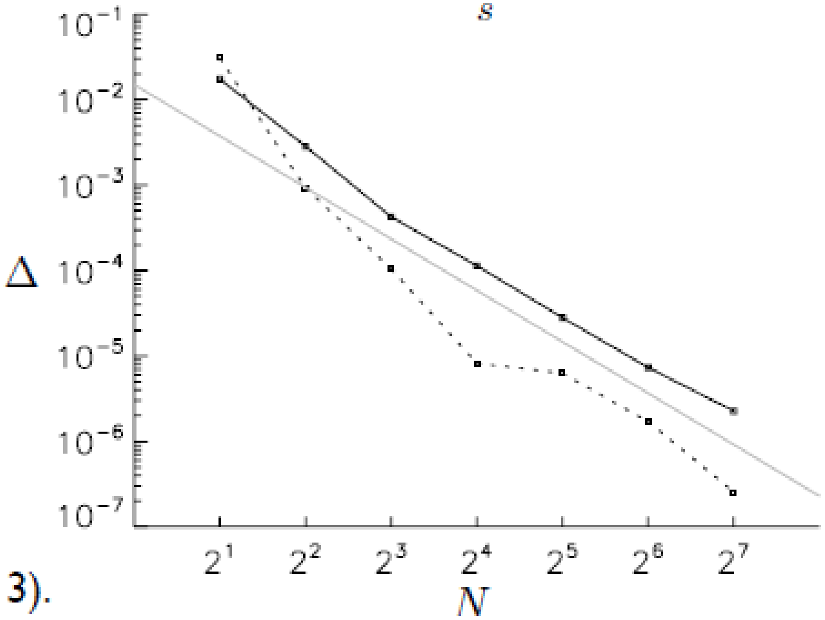

[1] G. Dennis *et al.*, *Phys. Plasmas* **20**, 032509 (2013).

Stepped Pressure Equilibrium Code, SPEC

[Hudson et al Phys. Plasmas 19, 112502 (2012)] Hudson

Vector potential is discretised using mixed Fourier & finite elements

- Coordinates (s,φ, ζ)
- Interface geometry $R_i = \sum_{l,m,n} R_{lmn} \cos(m\vartheta - n\zeta), \; Z_i = \sum_{l,m,n} Z_{lmn} \sin(m\vartheta - n\zeta)$
- Exploit gauge freedom $\mathbf{A} = A_\vartheta(s,\vartheta,\zeta)\nabla\vartheta + A_\zeta(s,\vartheta,\zeta)\nabla\zeta$
- Fourier $A_\vartheta = \sum_{m,n} \alpha(s)\cos(m\vartheta - n\varsigma)$
- Finite-element $a_\vartheta(s) = \sum_i a_{\vartheta,i}(s)\varphi(s)$

& inserted into constrained-energy functional $F = \sum_{l=1}^{N}(W_l - \mu_l H_l / 2)$

- Derivatives wrt **A** give Beltrami field $\nabla \times \mathbf{B} = \mu \mathbf{B}$
- Field in each annulus computed independently, distributed across multiple cpu’s
- Field in each annulus depends on enclosed toroidal flux, poloidal flux, interfaces ξ

Force balance solved using multi-dimensional Newton method

- Interface geometry adjusted to satisfy force balance $\mathbf{F}[\xi] = \{[[p + B^2/2]]_{m,n}\} = 0$
- Angle freedom constrained by spectral condensation,
- Dertivative matrix ∇F[ξ] computed in parallel using finite difference

Example: DIIID with n=3 applied error field

[Hudson et al Phys. Plasmas 19, 112502 (2012)]

Hudson

- 3D boundary, p, q-profile from STELLOPT reconstruction [*Sam Lazerson]*
- Irrational interfaces chosen to coincide with pressure gradients.

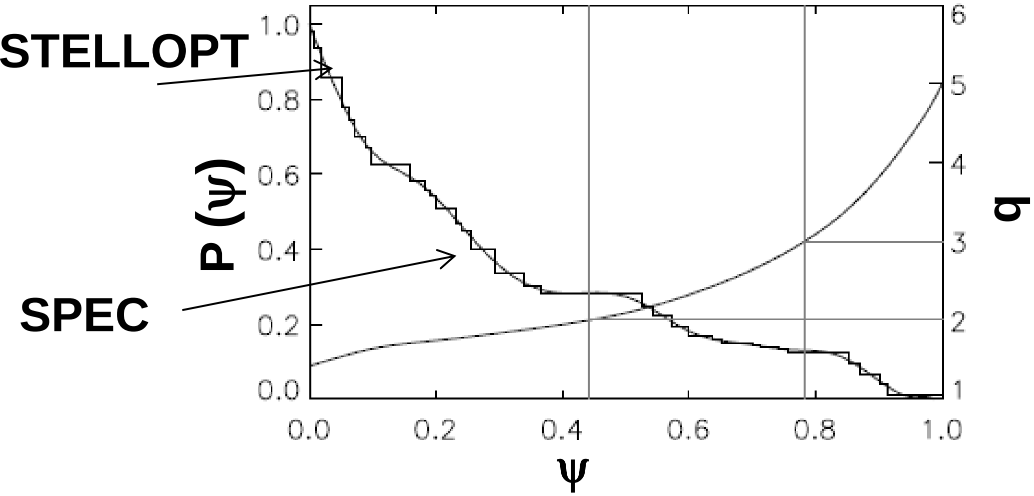

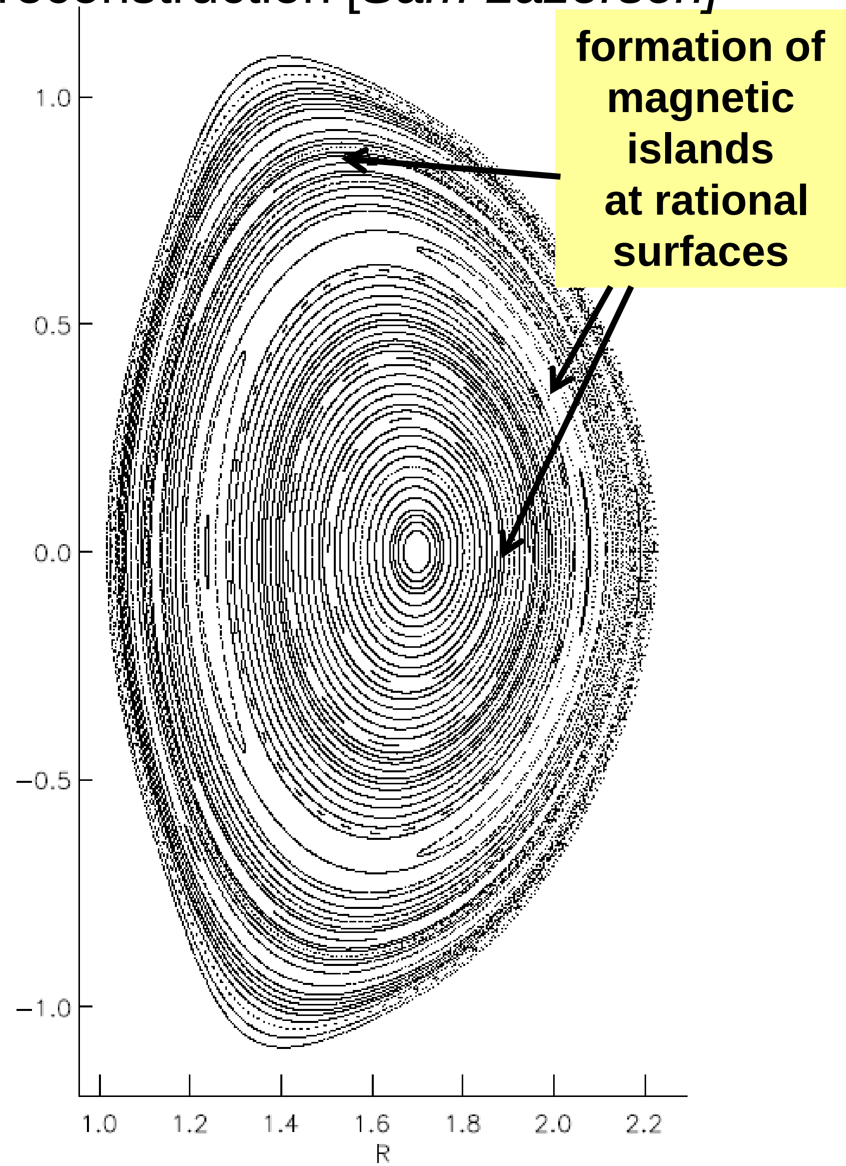

- Island formation is permitted
- No rational "shielding currents" included in calculation.

Spontaneously formed helical states

Dennis, Hudson, Terranova, Dewar, Hole, Escande

- The quasi-single helicity state is a stable helical state in RFP: becomes purer as current is increase

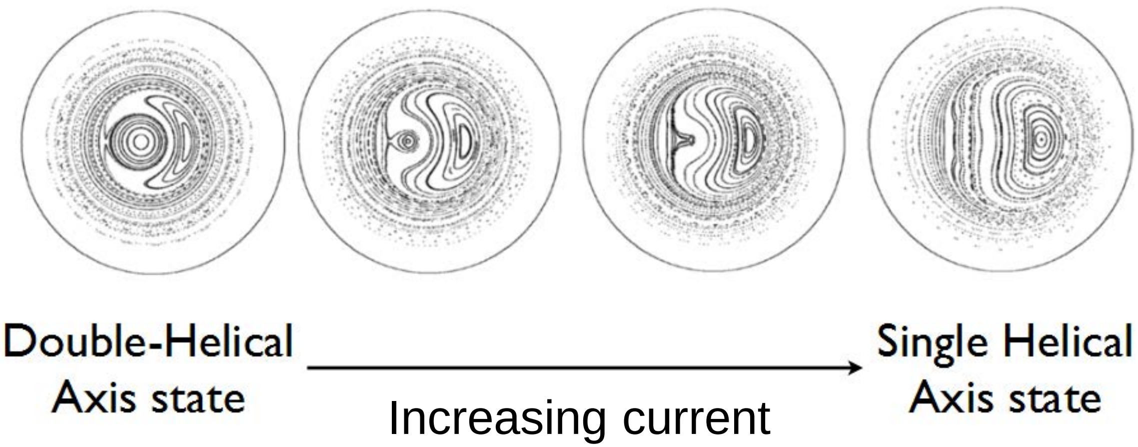

"Experimental" Poincaré plot

[Fig. 6 of P. Martin et al., Nuclear Fusion 49, 104019 (2009)]

Spontaneously formed helical states

Dennis, Hudson, Terranova, Dewar, Hole, Escande

- The quasi-single helicity state is a stable helical state in RFP: becomes purer as current is increase

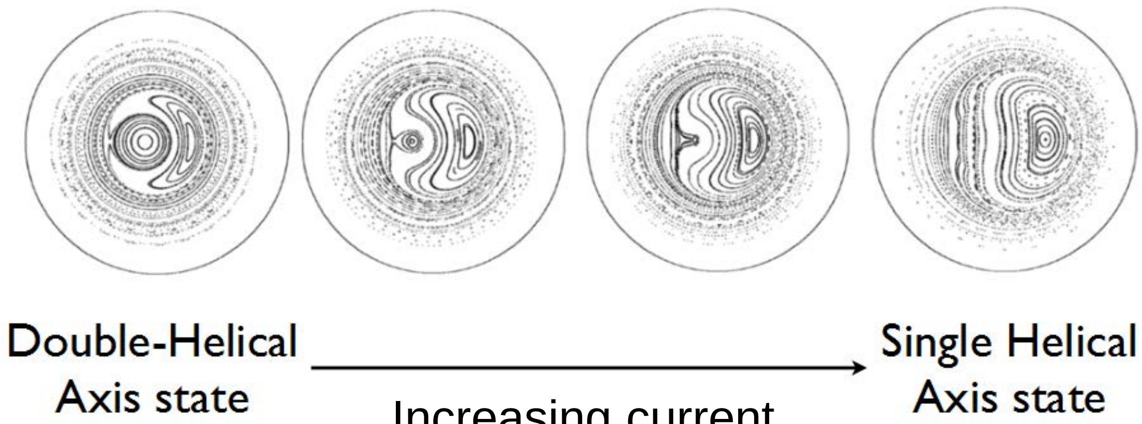

Increasing current

"Experimental" Poincaré plot

[Fig. 6 of P. Martin et al., Nuclear Fusion 49, 104019 (2009)]

- Ideal MHD with assumed nested flux surfaces can ***not*** model the DAX state

Spontaneously formed helical states

Dennis, Hudson, Terranova, Dewar, Hole, Escande

- The quasi-single helicity state is a stable helical state in RFP: becomes purer as current is increase

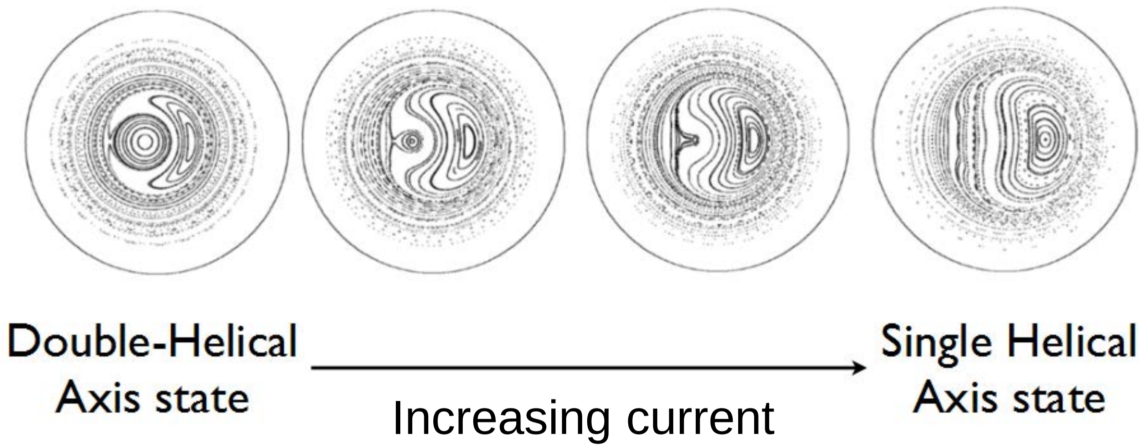

"Experimental" Poincaré plot

[Fig. 6 of P. Martin et al., Nuclear Fusion 49, 104019 (2009)]

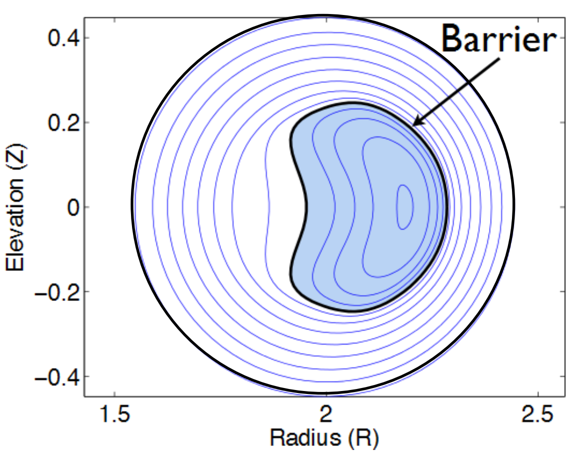

- Ideal MHD with assumed nested flux surfaces can ***not*** model the DAX state
- Might MRXMHD with 2 barriers offer a minimal description to describe DAX and SHAX states in the RFP?
- Model RFX-mod QSH state by a 2-interface minimum energy MRXMHD state.

[G. R. Dennis *et al* , Phys. Rev. Lett. **111**, 055003, 2013]

Plasma is a minimum energy state

- RFP bifurcated state has lower energy (preferred) than comparable axis-symmetric state

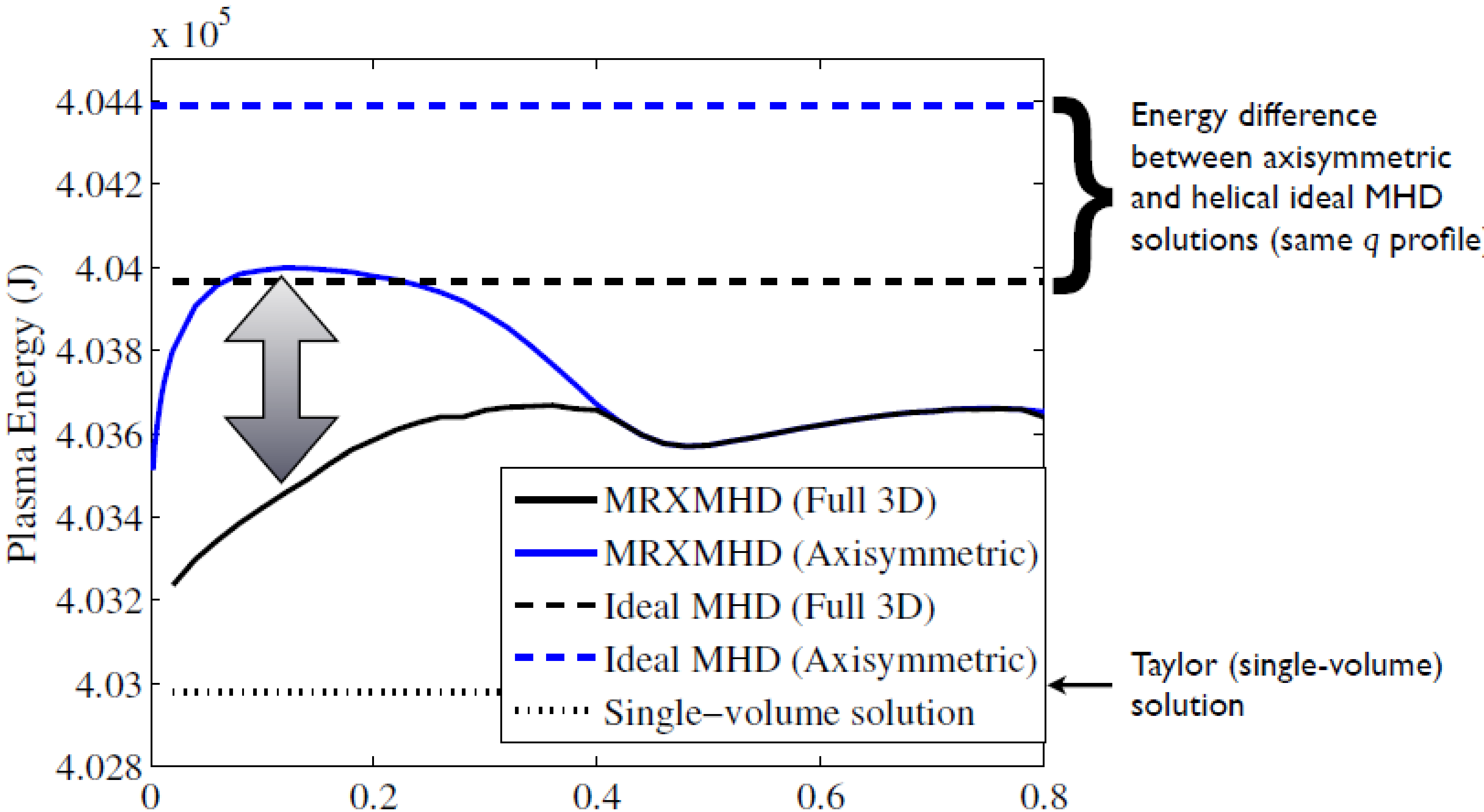

Ideal MHD flux surface chosen as ideal barrier

Spontaneously formed helical states

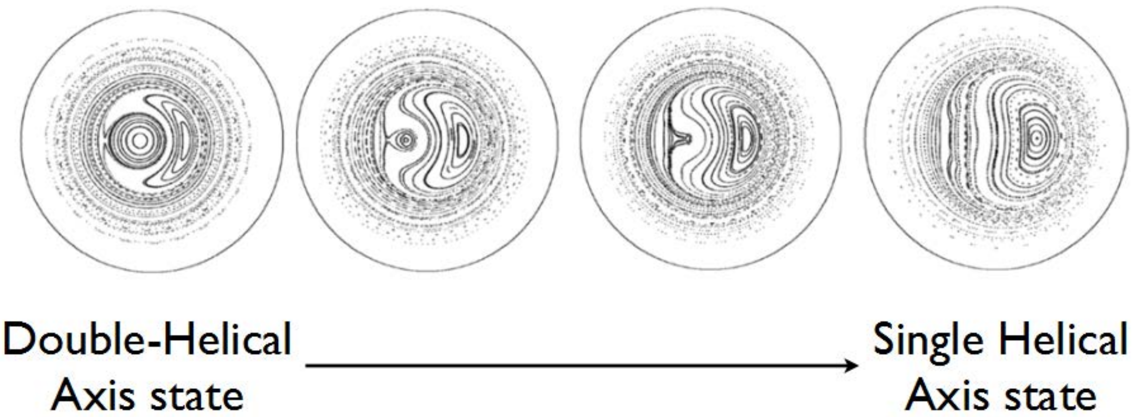

"Experimental" Poincaré plot

[Fig. 6 of P. Martin et al., Nuclear Fusion 49, 104019 (2009)]

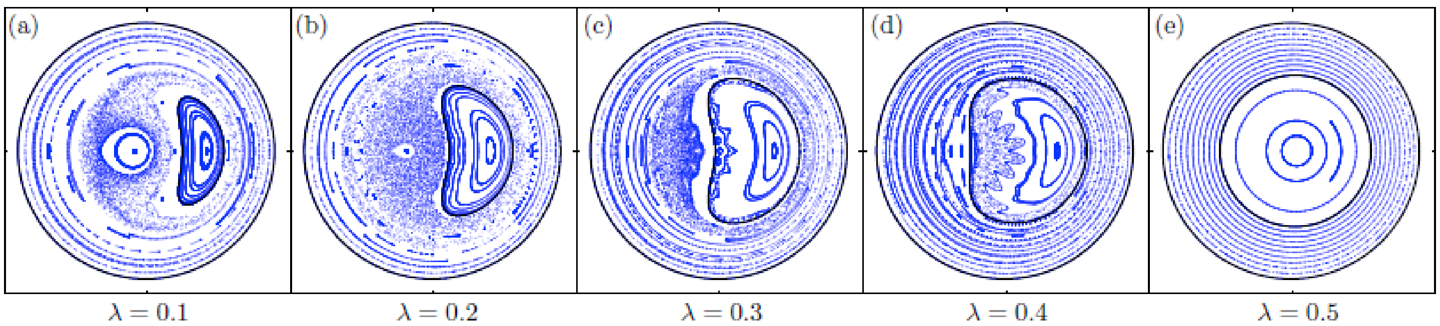

MRXMHD Poincaré plot G. R. Dennis PRL

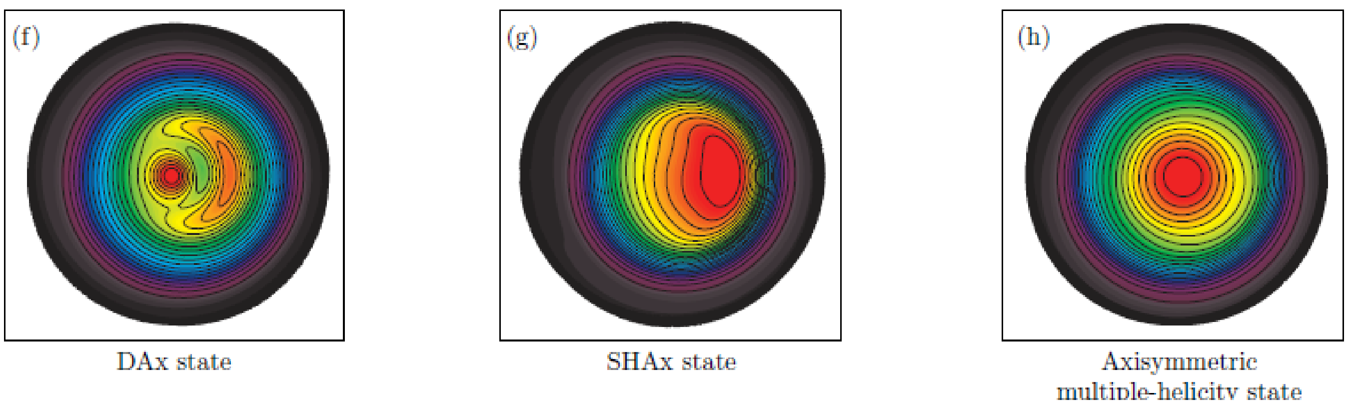

Soft X-ray data

Recent progress in MRxMHD

- Extended MRxMHD to include non-zero plasma flow and plasma anisotropy

  [G.R. Dennis, S.R. Hudson, R.L. Dewar, M.J. Hole, Phys. Plas. **21**, 042501 (2014)]

  [G.R. Dennis, S.R. Hudson, R.L. Dewar, M.J. Hole, Phys. Plas. **21**, 072512 (2014)]

- Generalized straight field line coordinates concept to fully 3D plasmas

  [R. L. Dewar, S. R. Hudson, A. Gibson, *Plasma Phys. Control. Fusion,* **55,** 014004, 2013]

- Related helical bifurcation of a Taylor relaxed state to a tearing mode

  [Z. Yoshida and R. L. Dewar , *J. Phys. A: Math. Theor.* **45**, 365502, 2012]

  [M. J. Hole, R. Mills, S. R. Hudson and R. L. Dewar Nucl. Fusion 49 (2009) 065019]

- Developed techniques to establish pressure jump a surface can support.

  [M. McGann, ANU PhD thesis, 2013]

Recent progress in MRxMHD

- Developed “plasmoids”, representing partial magnetic island chains
  [R. L. Dewar *et al*, Phys. Plas. **20**, 082103, 2013.]

- Computed the high-*n* stability of a pressure discontinuity in a 3D plasma.
  [D. Barmaz, ANU Masters Thesis 2011]

- Related ghost surfaces and isotherms in chaotic fields
  [S. R. Hudson and J. Breslau**,** Phys. Rev. Let., **100**, 095001, 2008]

Conclusions: Anisotropy and Flow

- Added anisotropy and toroidal flow to equilibrium reconstruction code EFIT TENSOR, and HELENA+ATF
- Developed new single adiabatic stability model which includes anisotropy and flow, reduces to ideal MHD as anisotropy and flow reduced
- Implemented Single Adiabatic CGL and incompressible stability treatments into continuum code CSMIS and stability code MISHKA-A
- Shown anisotropy changes the radial structure of TAE modes.

- *Does it change (wave-particle) anomalous transport?*
- *Explore the impact of anisotropy and flow on a wide range of MAST plasma conditions*

Conclusions: MRxMHD

- Introduced/ motivated multi-region relaxed MHD, and SPEC 3D MHD code
- Demonstrated application of SPEC to describe DIIID plasma with an applied error field
- Applied MRxMHD to reverse field pinch, explained transition from a double helical-axis to single helical axis state as a sequence of minimum energy MRxMHD states.

- *Extend SPEC to free boundary, including vacuum region and external conductors*
    - *Enables calculation of stability to external modes and response due to Resonant Magnetic Perturbation (RMP) coils*
- *Explain helical states in MAST (e.g. long-lived modes), and sawtooth reconnection cycle*
- *Address stability of chaotic field configurations*

"MHD with anisotropy in velocity, pressure"

- Pressure different parallel and perpendicular to field due mainly to *directed* neutral beam injection

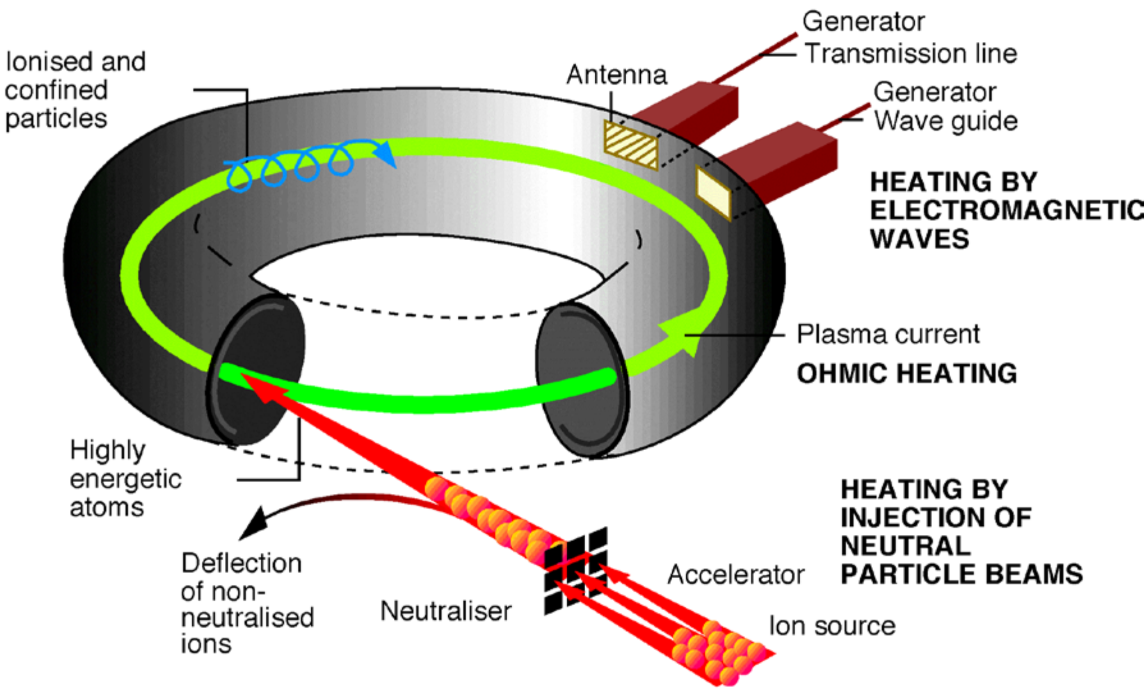

"MHD with anisotropy in velocity, pressure"

- Pressure different parallel and perpendicular to field due mainly to *directed* neutral beam injection

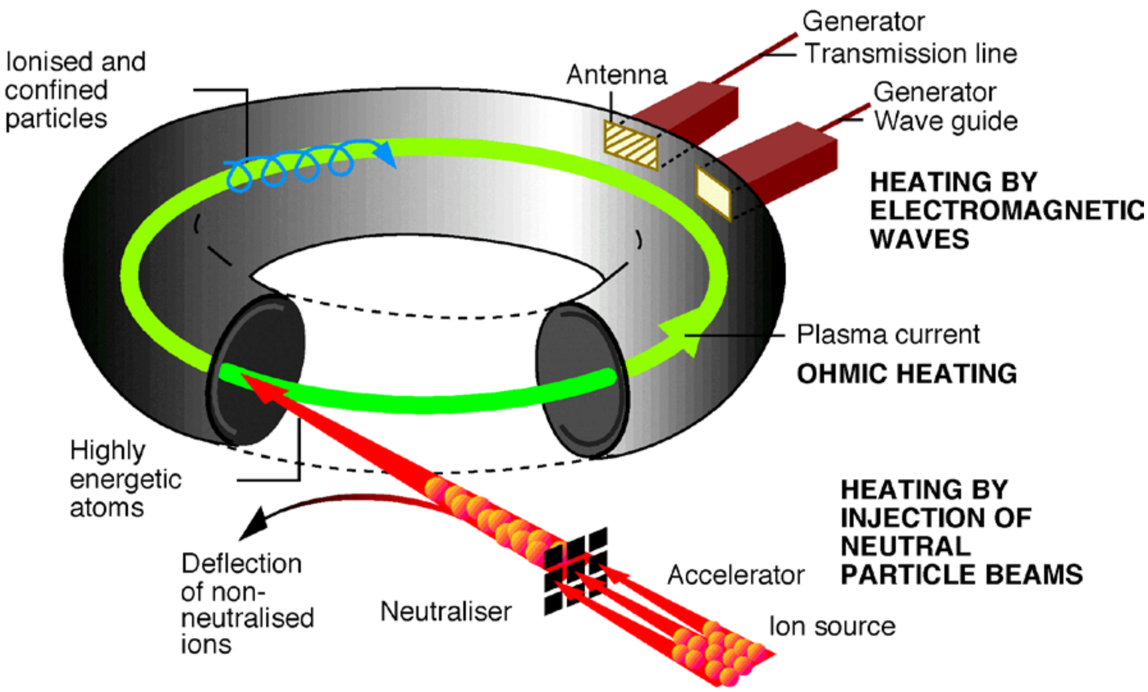

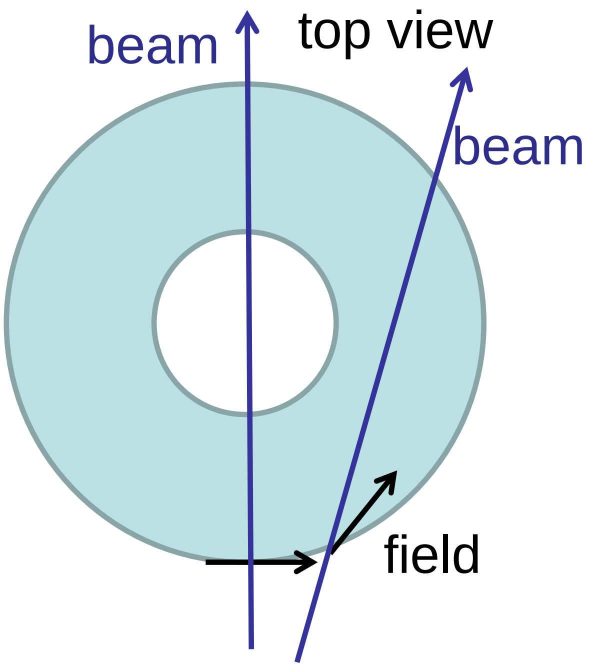

"MHD with anisotropy in velocity, pressure"

- Pressure different parallel and perpendicular to field due mainly to *directed* neutral beam injection

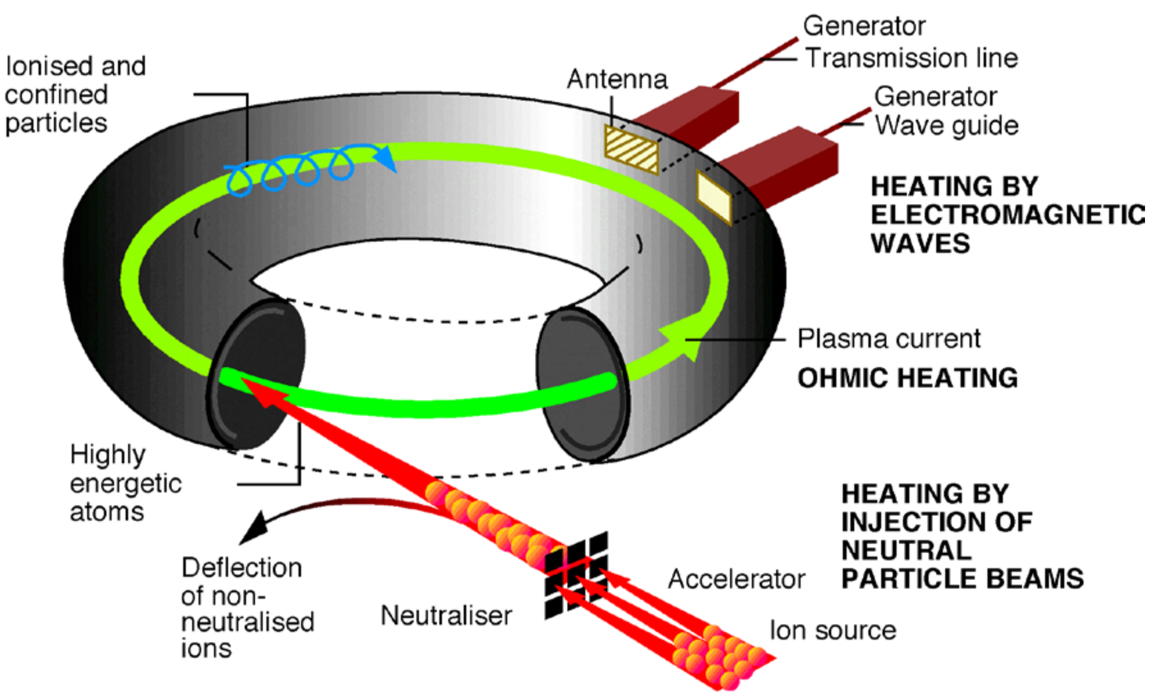

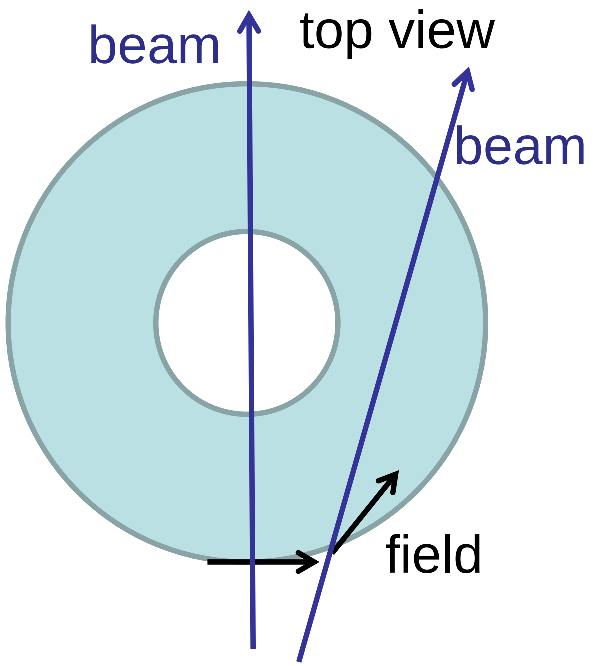

$\Rightarrow$ Pressure is a tensor $\quad \bar{\mathbf{P}} = p_{\perp}\bar{\mathbf{I}} + \Delta\mathbf{BB}/\mu_0\,, \qquad \Delta = \dfrac{\mu_0\left(p_{||} - p_{\perp}\right)}{B^2}$

Expected impact of anisotropy

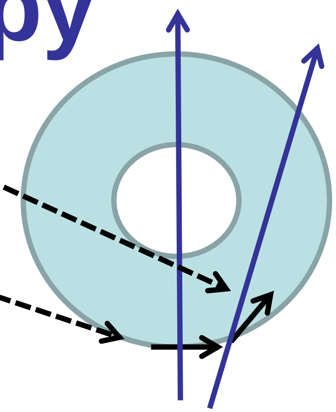

- Small angle θ_b between beam, field $\Rightarrow p_{||} > p_{\perp}$
- Beam orthogonal to field, $\theta_b=\pi/2 \Rightarrow p_{\perp} > p_{||}$
- If $p_{||}$ sig. enhanced by beam, $p_{||}$ surfaces distorted and displaced inward relative to flux surfaces

  [Cooper et al, Nuc. Fus. 20(8), 1980]

- If $p_{\perp} > p_{||}$, an increase will occur in centrifugal shift :

  [R. Iacono, A. Bondeson, F. Troyon, and R. Gruber, Phys. Fluids B 2 (8). August 1990]

- Obtain $p_{\perp}$ and $p_{||}$ from moments of distribution function, computed by TRANSP

Peaked pressure profile

Broad pressure profile

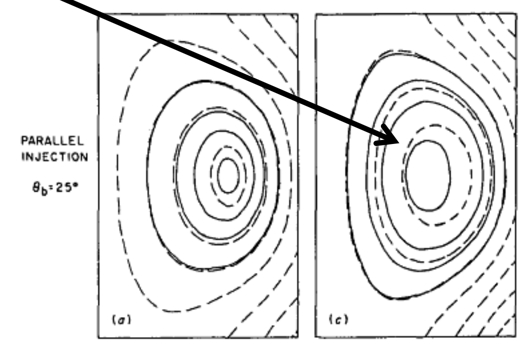

Parallel pressure contours(solid)

Flux surfaces (dashed)

[M J Hole, G von Nessi, M Fitzgerald, K G McClements, J Svensson, PPCF 53 (2011) 074021]

VMEC / SPEC comparison reveals chaos

Different toroidal cross-sections at λ = 0.4